Biochemical and Biophysical Research Communications 438 (2013) 193–197

Contents lists available at ScienceDirect

Biochemical and Biophysical Research Communications

journal homepage: www.elsevier.com/locate/ybbrc

Substrate binding to a GH131 β-glucanase catalytic domain from *Podospora anserina*

Tong Jiang [a,1], Hsiu-Chien Chan [a,1], Chun-Hsiang Huang [a], Tzu-Ping Ko [b], Ting-Yung Huang [c,d], Je-Ruei Liu [e], Rey-Ting Guo [a,*]

[a] Industrial Enzymes National Engineering Laboratory, Tianjin Institute of Industrial Biotechnology, Chinese Academy of Sciences, Tianjin 300308, China
[b] Institute of Biological Chemistry, Academia Sinica, Taipei 11529, Taiwan
[c] Genozyme biotechnology Inc., Taipei 106, Taiwan
[d] AsiaPac Biotechnology Co., Ltd., Dongguan 523808, China
[e] Institute of Biotechnology, National Taiwan University, Taipei 106, Taiwan

ARTICLE INFO

Article history:
Received 12 July 2013
Available online 20 July 2013

Keywords:
Glycoside hydrolase
Crystal structure
β-Glucanase
GH131

ABSTRACT

β-Glucanases have been utilized widely in industry to treat various carbohydrate-containing materials. Recently, the *Podospora anserina* β-glucanase 131A (PaGluc131A) was identified and classified to a new glycoside hydrolases GH131 family. It shows exo-β-1,3/exo-β-1,6 and endo-β-1,4 glucanase activities with a broad substrate specificity for laminarin, curdlan, pachyman, lichenan, pustulan, and cellulosic derivatives. Here we report the crystal structures of the PaGluc131A catalytic domain with or without ligand (cellotriose) at 1.8 Å resolution. The cellotriose was clearly observed to occupy the +1 to +3 subsites in substrate binding cleft. The broadened substrate binding groove may explain the diverse substrate specificity. Based on our crystal structures, the GH131 family enzyme is likely to carry out the hydrolysis through an inverting catalytic mechanism, in which E99 and E139 are supposed to serve as the general base and general acid.

1. Introduction

Lignocellulosic biomass is the most abundant source of energy from plants which contains carbohydrate molecules with various chemical linkages [1]. The hydrolysis of cellulose into monosaccharides required three major cellulolytic enzymes: endoglucanase, exoglucanase and β-glucosidase [2]. *Podospora anserina* has been demonstrated to possess one of the largest fungal sets of candidate enzymes (from CAZy website) for cellulose degradation [3], with one of the largest numbers of carbohydrate-binding modules (CBMs) among all of the fungal genomes [4].

In 2012, a new glycoside hydrolase (GH) was classified as GH131 family from *P. anserina* (PaGluc131A) [5]. PaGluc131A is composed of a catalytic domain at the N-terminal end, a carbohydrate-binding module family 1 (CBM1) domain at the C-terminal end, and a linker that connects the two domains. Although the function of CBM1 domain for GH131 members remains unclear, the CBM1 domain is essential for the enzyme activity [5]. PaGluc131A has drawn much attentions because it is an unusual hydrolase and can act on a broad range of β-glucan polysaccharides, including laminarin, curdlan, pachyman, lichenan, pustulan, and cellulosic derivatives. Furthermore, it was also proved as a bi-functional enzyme possessing activities of exo-β-1,3/exo-β-1,6 and endo β-1,4 glucanase.

More recently, the crystal structure of the catalytic domain of GH131 from a basidiomycete fungus *Coprinopsis cinerea* (CcGH131A) was solved [6]. The structure of CcGH131A features a β-jelly roll fold. Based on the CcGH131A structure, four critical residues (R96, E98, E138 and H218) were predicted to play important roles in catalysis. However, the proposed mechanism needs to be further verified using complex structures containing real substrate/product, instead of glycerol molecules. Here we solved the crystal structures of the catalytic domain of Gluc131A from *P. anserina* in apo-form and in complex with cellotriose at high resolution. Our results clearly identified the substrate binding pocket of PaGluc131A, and revealed the detailed interaction networks between the ligand and active site residues. The molecular mechanism of the novel GH131 family is now clearly elucidated, with an inverting mechanism proposed accordingly.

2. Materials and methods

2.1. Expression and purification of PaGluc131A-270

The gene encoding of catalytic domain (residues 1–270) of *Gluc131A* (*PaGluc131A-270*) from *P. anserina* was synthesized

* Corresponding author.
E-mail address: guo_rt@tib.cas.cn (R.-T. Guo).
[1] These authors contributed equally to this work.

0006-291X/$ - see front matter © 2013 Elsevier Inc. All rights reserved.
http://dx.doi.org/10.1016/j.bbrc.2013.07.051

chemically and amplified by polymerase chain reaction (PCR) with forward primer 5′- GGTATTGAGGGTCGCGAAAACCTGTATTTTCAG GGTGCGGGTGCGGGTGCGGGAACTATTTTGTGGGATGGAAGATTT-3′ and reverse primer 5′-AGAGGAGAGTTAGAGCCATTATTTTTCAAAC TGCGGATGAGACCACGCAGACGCCGCCGCCAAACATTGAGAGTACCA GTCGTTACC-3′, and then cloned into the pET32 Xa/LIC vector. The recombinant plasmids were transformed to *E. coli* BL21 (DE3) trxB and the protein was induced with 0.5 mM isopropyl-thiogalactopyranoside (IPTG) at 30 °C for 12 h.

Cell paste was harvested by centrifugation at 7000×*g* and resuspended in a lysis buffer containing 25 mM Tris–HCl, pH 7.5, 150 mM NaCl and 20 mM imidazole. Cell lysate was prepared with a French Press Instrument (GuangZhou JuNeng Biology&Technology Co., LTD), and then centrifuged at 17000×*g* to remove cell debris. The proteins were purified by FPLC using a Ni–NTA column. The buffer and gradient for the Ni–NTA column were 25 mM Tris–HCl, pH 7.5, 150 mM NaCl, and 20–250 mM imidazole. His-tagged PaGluc131A-270 was eluted at about 125 mM imidazole. The protein solution was dialyzed against a buffer containing 25 mM Tris–HCl, pH 7.5 and then purified by FPLC using DEAE column, the buffer and gradient for the DEAE column were 25 mM Tris–HCl, pH 7.5, and 0–500 mM NaCl. The protein was eluted at about 250 mM NaCl. And the protein solution was dialyzed against another buffer containing 25 mM Tris–HCl, pH 7.5, 150 mM NaCl and then subjected to Tev protease digestion to remove the His tag and thioredoxin fusion protein. The mixture was then passed through Ni–NTA column again and the untagged PaGluc131A-270 was eluted with non-imidazole-containing buffer. Selenomethionine (SeMet) protein was obtained by using a simple minimal medium with some salts and L-SeMet [7]. The preparation procedure of the SeMet-substituted protein was similar to that of the wild-type protein.

2.2. Crystallization, data collection, structure determination and refinement

Prior to crystallization, the purified PaGluc131A-270 and SeMet protein were concentrated to 25 mg/ml in 25 mM Tris–HCl, 150 mM NaCl, pH 7.5 buffer. The wild-type PaGluc131A-270 protein was first crystallized by using the PEG/LiCl screen kit (Hampton Research) and sitting-drop vapor diffusion method. The D4 reservoir solution contained 0.1 M HEPES, pH 7.0, 1 M LiCl and 30% w/v PEG6000. Better crystals were obtained at 0.1 M HEPES, pH 7.0, 0.7 M LiCl and 33% PEG6000. The SeMet protein crystal was obtained in 0.1 M HEPES, pH 7.0, 0.5 M LiCl and 32% PEG6000. All crystals were prepared at room temperature and reached suitable size for data collection in 7 days. The cellotriose-bound crystal was obtained by soaking the native crystal with mother liquor containing 10 mM cellotriose for 3 h.

The X-ray diffraction datasets from the SeMet, apo-form and the complex (PaGluc131A-270-cellotriose) crystals were collected at 1.80 to 1.93 Å resolution at beam line BL13B1 and BL13C1 of the National Synchrotron Radiation Research Center (NSRRC, Hsinchu, Taiwan). There is no need for preparing the crystal cryoprotecant, because the PEG6000 concentration is high enough to be cryoprotectant during data collection. All of these datasets were processed using the program HKL2000 [8]. The crystals belong to the space group *P*1 and there are four molecules in an asymmetric unit. Prior to use in structural refinements, 5% randomly selected reflections were set aside for calculating R_{free} as a monitor [9]. The initial phase information was derived from single-wavelength anomalous diffraction (SAD) method. The Se sites were first found by SHLEXD [10] and then refined by SOLVE [11]. Subsequently, the initial phase was significantly enhanced by *OASIS*-aided SAD phasing and phase-improvement process [12]. The final initial model containing 969 residues with side-chains was built by RESOLVE [11] and ARP/wARP [13]. The following native data set was refined at 1.8 Å resolution using CNS [14] and Coot [15] programs. The complex structure (PaGluc131A-270-cellotriose) was determined by molecular replacement (MR) method with PHASER [16] by using the refined apo-structure as a search model. The $2F_o-F_c$ difference Fourier map showed clear electron densities for most amino acid residues. Subsequent refinements by incorporating water molecules and ligands were according to 1.0 map level by using CNS [14] and Coot [15]. Data collection and refinement statistics of these crystals are summarized in Table 1. All figures were prepared by using PyMOL (http://pymol.sourceforge.net/).

Table 1
Summary of data processing and refinement statistics.

G3 = Cellotriose	Se-Met (Peak)	Native	G3-soak
PDB code		4LE3	4LE4
Data collection			
Space group	*P*1	*P*1	*P*1
Wavelength (Å)	0.97919	1.00000	0.97622
Unit-cell parameters			
a/b/c (Å)	55.2/62.5/79.4	54.8/62.2/79.2	54.6/61.9/79.0
α/β/γ (°)	81.8/74.9/77.3	81.6/75.0/77.1	81.5/75.2/77.3
Resolution (Å)	25.0–1.93 (2.00–1.93)	25.0–1.80 (1.86–1.80)	25.0–1.80 (1.86–1.80)
Unique reflections	71890 (6995)	86955 (8620)	87110 (8638)
Redundancy	4.3 (3.7)	3.0 (3.1)	3.4 (3.3)
Completeness (%)	96.4 (93.3)	96.2 (95.4)	97.0 (95.9)
Average I/σ(I)	16.5 (2.6)	19.6 (4.3)	17.9 (3.0)
R_{merge} (%)	8.9 (36.9)	6.9 (29.7)	6.9 (29.7)
Refinement			
No. of reflections		85623 (7873)	84769 (7674)
R_{work} (95% of data)		0.176 (0.233)	0.178 (0.256)
R_{free} (5% of data)		0.217 (0.279)	0.216 (0.304)
R.m.s.d. bonds (Å)		0.010	0.012
R.m.s.d. angles (°)		1.674	1.630
Dihedral angles (%)			
Most favored		87.3	87.9
Allowed		12.5	11.9
Disallowed		0.2	0.2
Average B (Å^2)/No. of non-H atoms			
Protein		22.9/7707	19.7/7702
Water		39.8/1300	34.2/1126
Ligand			52.1/34

Values in parentheses are for the highest resolution shell.

2.3. PDB accession numbers

The atomic coordinates and structure factors of the PaGluc131A-270 in apo-form and in complex with cellotriose have been deposited in the RCSB Protein data bank, with the accession code 4LE3 and 4LE4, respectively.

3. Results and discussion

3.1. Overall structures

Single-wavelength anomalous diffraction (SAD) data of SeMet crystal was collected to solve the PaGluc131A-270 structure because at that time no GH131 structure was available for structure determination otherwise. Most recently, a catalytic domain structure of *C. cinerea* GH131A (PDB code: 3W9A) was determined. The catalytic domain protein sequence identity is 52% compared to PaGluc131A-270 (whole protein sequence identity is 43%) [6].

There are four molecules in an asymmetric unit of the PaGluc131A-270 crystal. A PDBePISA [17] analysis demonstrated that both apo- and ligand-bound forms are monomeric enzyme, because it lacks significant surface contacts or interactions with the

other monomers. All monomers seen in the crystals are continuous from the N- to C-terminus (residues 19–267 for A chain; 19–263 for B chain; 19–260 for C chain; 19–265 for D chain), except for the last few C-terminal residues being missing. These four PaGluc131A-270 apo structures are very similar and the root-mean-square derivations (RMSD) of all Cα-atoms are 0.16 Å to 0.22 Å. Among the four monomers in the complex crystal, only one monomer was found to contain a cellotriose density. By comparing the apo and complex structures, there is no significant conformational changes (RMSD is 0.082 Å for 225 Cα-atoms). However, the putative catalytic residue E139 has its side chain oriented differently upon cellotriose binding (Figure S1).

The overall structure of PaGluc131A-270 in complex with cellotriose is shown in Fig. 1A. The structure adopts a jelly-roll fold, which includes nine outer β strands (A1-A9) and six inner β strands (B1-B6) (Fig. 1B). The β-sheets A and B are packed against each other and linked by interconnecting loops. The active-site cleft is formed by inner β-sheet B and its associated loops (Fig. 1C). In comparison with the other jelly-roll fold proteins (GH7, GH11, GH12, and GH16), the β-sheet B is less bent and the overall length is shorter, so that the active site region forms a shallow and wide cleft [18]. Because the PaGluc131A was the first enzyme classified into GH131 family, many hypothetic proteins based on the sequence homology have also been identified. Recently, the crystal structure of the N-terminal domain of GH131 protein from *C. cinerea* was solved. The catalytic domain of PaGluc131A shares a sequence identity of 52% with that of CcGH131A, and the putative active-site residues are highly conserved (Figure S2). The RMSD between PaGluc131A-270 and CcGH131A is 1.2 Å for 235 Cα atoms, with major difference lying in the connecting loops (Figure S3). All of the β-strands of PaGluc131A-270 are shorter than those of CcGH131A, and one additional β-strand in the inner sheet B was observed in CcGH131A.

3.2. The substrate-binding site

There is only one cellotriose (CTR) observed in one of the four polypeptide chains in an asymmetric unit but the electron density is very clear (Fig. 1D). The CTR was found to occupy subsites +1 to +3. The detailed interactions between PaGluc131A-270 and CTR are depicted in Fig. 2A. One carboxyl oxygen atom of E139 made an H-bond of 2.9 Å to the O4 atom of +1 sugar. The other carboxyl oxygen atom of E139 formed two hydrogen bonds with the O3 atom of +1 sugar at 2.7 Å, and with the side chain NE2 of H224 at 3.3 Å. The ND1 atom of H224 also formed an H-bond with E99. Therefore, H224 probably is stabilized in a protonated form. E99 is also hydrogen bonded to R97, which in turn stabilizes the O3 atom of +1 sugar by a hydrogen bond and mediates a water molecule to interact with the O4 atom of +1 sugar. I52 and W90 provide nonpolar interactions to the sugar ring. W41 provides stacking force with the +3 sugar and Y51 formed one hydrogen bond of 3.4 Å with the O4 of +2 sugar. Previous kinetic studies showed that PaGluc131A can hydrolyze both β-(1,3)/(1,6) and barely β-(1,4) linked substrates [5]. Based on our complex

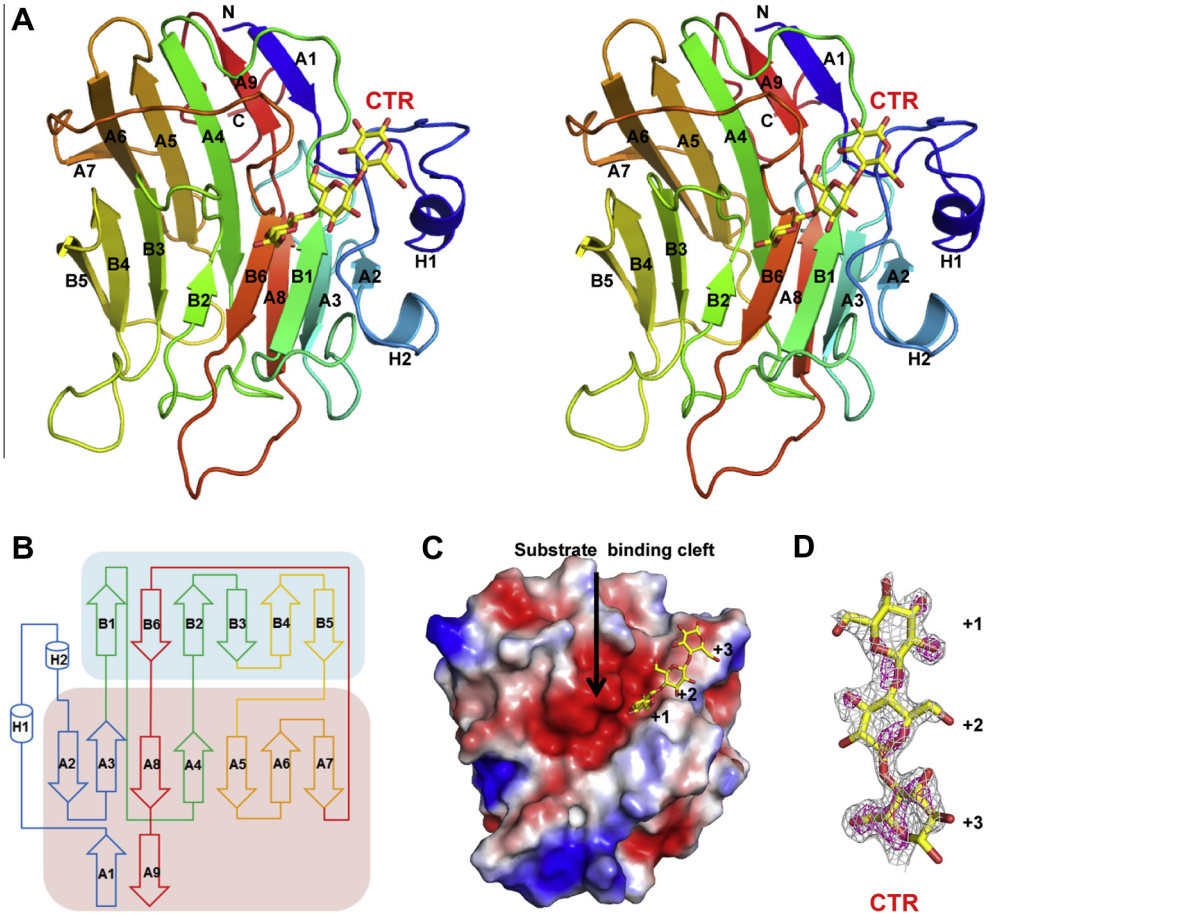

Fig. 1. Overall structure of PaGluc131A-270 in complex with cellotriose. (A) Stereo-view of complex structure of PaGluc131A-270 with cellotriose (CTR). The secondary structural elements and loops are spectrum-colored from N-terminus (blue color) to C-terminus (red). (B) The topology is depicted as a schematic diagram. (C) Electrostatic surface view of PaGluc131A-270 structure. The CTR molecule is shown as yellow sticks. (D) The 2Fo-Fc maps of CTR are contoured at 1 and 1.5 σ level and colored in gray and red, respectively. Subsites are numbered. (For interpretation of color in Fig. 1 the reader is referred to the web version of this article.)

structure, the protein surface model revealed that the active site possesses a shallower and wider substrate-binding shape which might be able to accommodate various kind of polysaccharides (Fig. 1C). In addition, fewer interactions between the ligand and active site residues of PaGluc131A-270 were observed comparing to other glucanases with narrow substrate specificity, which generally is a result of more interactions between enzyme and ligand.

3.3. Proposed catalytic mechanism

Because the CTR in the complex structure was observed in +1 to +3 sites, it was hard to define the anomeric atom. Compared with the three glycerol molecules in the CcGH131A structure, the +1 sugar of CTR was near Gol-C (Fig. 2B). Based on the complex structure of PaGluc131A-270 with CTR, the four highly conserved GH131A residues, R97, E99, E139, and H224 are located in the active site. To better understand the detailed catalytic mechanism, a cellotetraose (CTT) was modeled into PaGluc131A structure in the −1 to +3 subsites (Figure S4). From the previous CcGH131A structure, a catalytic dyad of E98 and H218 (corresponding to E99 and H224 in PaGluc131A-270) was proposed [19,20]. It represents an unusual catalytic machinery in which H218 acts as a catalytic residue and E98 activates the histidine during catalysis. The catalytic dyad acts as both acid and base in a retaining enzyme but as an acid in the inverting enzyme. However, the dyad E99-H224 in PaGluc131A-270 (corresponding to E98-H218 in CcGH131A) is not properly positioned for catalysis.

From our structure, the E139 side chain which makes hydrogen bonds to both O3 and O4 atoms of the +1 sugar of CTT is most likely to act as the general acid. It is in a good position for proton donor. The close vicinity to both O3 and O4 explains the dual specificity in cleaving β-1,3 and β-1,4 bonds. The adjacent H224 can relay its proton and keep E139 in a protonated state. Regarding the general base, E99 on the opposite side of E139 seems to be the best candidate. The distance between the carboxylate oxygen atoms of E99 and E139 is ~9 Å, suggesting that PaGluc131A-270 is an inverting enzyme. Because of its relative position and distance to the C1 atom of −1 sugar of CTT (>4 Å; Figure S4), E99 can effectively deprotonate a water molecule and direct it toward the anomeric carbon for nucleophilic attack. In addition, the adjacent positively charged R97 can keep E99 in a deprotonated state. These observations suggest that the GH131 enzymes might adopt an inverting

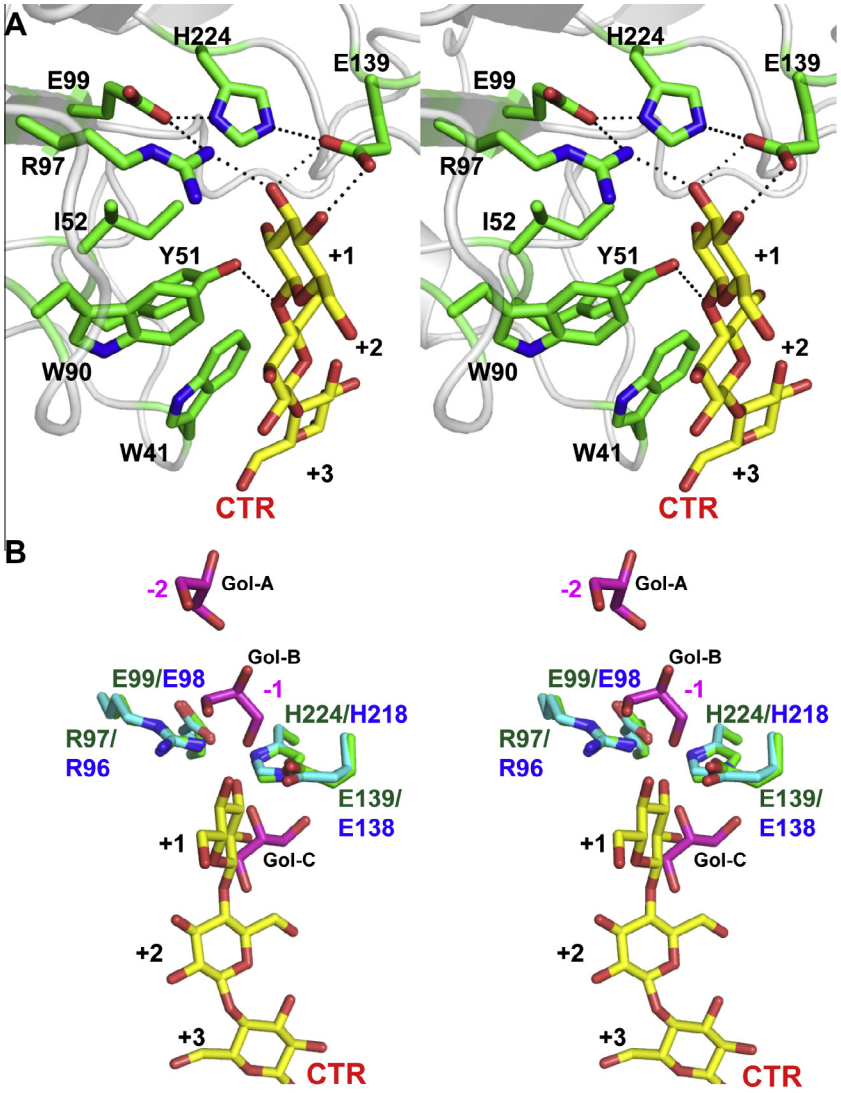

Fig. 2. Detail interaction in the active site. (A) The interaction of PaGluc131A-270 with bound CTR. CTR is shown in yellow stick and labeled from +1 to +3 subsites. The active-site residues are colored in green stick. The hydrogen bonds are shown in black dash lines. (B) Stereo-view of the superimposed active-site residues of the PaGluc131A-270 with CTR and CcGH131A with three glycerols. The residues in the active sites from PaGluc131A-270 and CcGH131A are colored in green and cyan, and the CTR and three glycerols are colored in yellow and pink, respectively. (For interpretation of color in Fig. 2 the reader is referred to the web version of this article.)

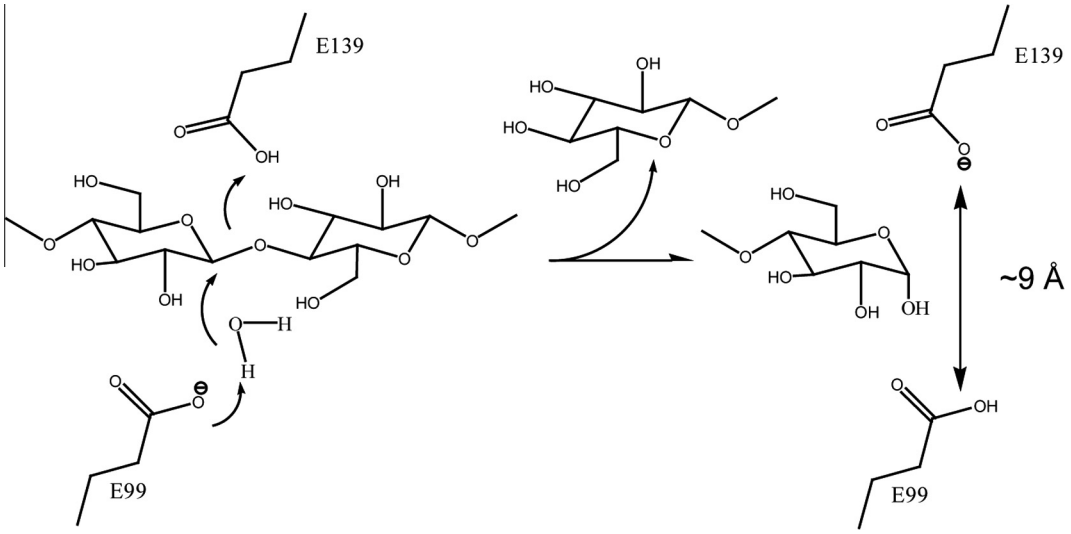

Fig. 3. Proposed catalytic mechanism of PaGluc31A-270. The reaction of an inverting enzyme is depicted in a schematic diagram. The two glucose residues correspond to those bound to the −1 and +1 subsites. Here E99 acts as general base and E139 acts as general acid.

mechanism [21], with E99 acting as the general base and E139 as the general acid. (see Figs. 1 and 2)

In conclusion, our complex structure provides more evidence to clarify the mechanism of GH131A family. The inverting reaction mechanism is proposed in Fig. 3. E99 is the general base to activate a water to attack the C1 atom of the −1 sugar ring. E139 serves as the general acid to facilitate the glycosidic bond cleavage and the leaving of +1 sugar. In our crystal, the E139 side chain directly interacts with the O3 and O4 atoms, but not O6. Overall, this study gives detailed interactions at the active site of a GH131 family enzyme in complex with a carbohydrate.

Acknowledgments

This work was supported by National High Technology Research and Development Program of China (2012AA022200), National Basic Research Program of China (2011CB710800 and 2011CBA00805) and Tianjin Municipal Science and Technology Commission (12ZCZDSY12500). We thank the National Synchrotron Radiation Research Center of Taiwan for beam–time allocation and data–collection assistance.

Appendix A. Supplementary data

Supplementary data associated with this article can be found, in the online version, at http://dx.doi.org/10.1016/j.bbrc.2013.07.051.

References

[1] A.L. Demain, M. Newcomb, J.H. Wu, Cellulase, clostridia, and ethanol, Microbiol. Mol. Biol. Rev. 69 (2005) 124–154.
[2] M.K. Bhat, S. Bhat, Cellulose degrading enzymes and their potential industrial applications, Biotechnol. Adv. 15 (1997) 583–620.
[3] B.L. Cantarel, P.M. Coutinho, C. Rancurel, T. Bernard, V. Lombard, B. Henrissat, The Carbohydrate-active enzymes database (CAZy): an expert resource for glycogenomics, Nucleic Acids Res. 37 (2009) D233–238.
[4] E. Espagne, O. Lespinet, F. Malagnac, C. Da Silva, O. Jaillon, B.M. Porcel, A. Couloux, J.M. Aury, B. Segurens, J. Poulain, V. Anthouard, S. Grossetete, H. Khalili, E. Coppin, M. Dequard-Chablat, M. Picard, V. Contamine, S. Arnaise, A. Bourdais, V. Berteaux-Lecellier, D. Gautheret, R.P. de Vries, E. Battaglia, P.M. Coutinho, E.G. Danchin, B. Henrissat, R.E. Khoury, A. Sainsard-Chanet, A. Boivin, B. Pinan-Lucarre, C.H. Sellem, R. Debuchy, P. Wincker, J. Weissenbach, P. Silar, The genome sequence of the model ascomycete fungus *Podospora anserina*, Genome Biol. 9 (2008) R77.
[5] M. Lafond, D. Navarro, M. Haon, M. Couturier, J.G. Berrin, Characterization of a broad-specificity beta-glucanase acting on beta-(1,3)-, beta-(1,4)-, and beta-(1,6)-glucans that defines a new glycoside hydrolase family, Appl. Environ. Microbiol. 78 (2012) 8540–8546.
[6] T. Miyazaki, M. Yoshida, M. Tamura, Y. Tanaka, K. Umezawa, A. Nishikawa, T. Tonozuka, Crystal structure of the N-terminal domain of a glycoside hydrolase family 131 protein from *Coprinopsis cinerea*, FEBS Lett. (2013).
[7] S.A. Guerrero, H.J. Hecht, B. Hofmann, H. Biebl, M. Singh, Production of selenomethionine-labelled proteins using simplified culture conditions and generally applicable host/vector systems, Appl. Microbiol. Biotechnol. 56 (2001) 718–723.
[8] Z. Otwinowski, W. Minor, Processing of X-ray diffraction data collected in oscillation mode, Methods in Enzymol. 276 (1997) 307–326.
[9] A.T. Brunger, Assessment of phase accuracy by cross validation: the free R value. Methods and applications, Acta. Crystallogr. D Biol. Crystallogr. 49 (1993) 24–36.
[10] T.R. Schneider, G.M. Sheldrick, Substructure solution with SHELXD, Acta. Crystallogr. D Biol. Crystallogr. 58 (2002) 1772–1779.
[11] T.C. Terwilliger, SOLVE and RESOLVE: automated structure solution and density modification, Methods Enzymol. 374 (2003) 22–37.
[12] T. Zhang, Y. He, J.W. Wang, L.J. Wu, C.D. Zheng, Q. Hao, Y.X. Gu, H.F. Fan, OASIS4.2 - a computer program of direct-method phase extension for proteins. Institute of Physics, Chinese Academy of Sciences, P.R. China, 2012, (http://cryst.iphy.ac.cn).
[13] A. Perrakis, R. Morris, V.S. Lamzin, Automated protein model building combined with iterative structure refinement, Nat. Struct. Biol. 6 (1999) 458–463.
[14] A.T. Brunger, P.D. Adams, G.M. Clore, W.L. DeLano, P. Gros, R.W. Grosse-Kunstleve, J.S. Jiang, J. Kuszewski, M. Nilges, N.S. Pannu, R.J. Read, L.M. Rice, T. Simonson, G.L. Warren, Crystallography & NMR system: A new software suite for macromolecular structure determination, Acta. Crystallogr. D Biol. Crystallogr. 54 (1998) 905–921.
[15] P. Emsley, K. Cowtan, Coot: model-building tools for molecular graphics, Acta. Crystallogr. D Biol. Crystallogr. 60 (2004) 2126–2132.
[16] A.J. McCoy, R.W. Grosse-Kunstleve, P.D. Adams, M.D. Winn, L.C. Storoni, R.J. Read, Phaser crystallographic software, J. Appl. Crystallogr. 40 (2007) 658–674.
[17] E. Krissinel, K. Henrick, Inference of macromolecular assemblies from crystalline state, J. Mol. Biol. 372 (2007) 774–797.
[18] Y.-S. Cheng, T.-P. Ko, T.-H. Wu, Y. Ma, C.-H. Huang, H.-L. Lai, A.H.J. Wang, J.-R. Liu, R.-T. Guo, Crystal structure and substrate-binding mode of cellulase 12A from *Thermotoga maritima*, Proteins Struct. Funct. Bioinform. 79 (2011) 1193–1204.
[19] S. Litzinger, S. Fischer, P. Polzer, K. Diederichs, W. Welte, C. Mayer, Structural and kinetic analysis of *Bacillus subtilis* N-acetylglucosaminidase reveals a unique Asp-His dyad mechanism, J. Biol. Chem. 285 (2010) 35675–35684.
[20] J.H. Hehemann, L. Smyth, A. Yadav, D.J. Vocadlo, A.B. Boraston, Analysis of keystone enzyme in Agar hydrolysis provides insight into the degradation (of a polysaccharide from) red seaweeds, J. Biol. Chem. 287 (2012) 13985–13995.
[21] G. Davies, B. Henrissat, Structures and mechanisms of glycosyl hydrolases, Structure 3 (1995) 853–859.